Available online at www.sciencedirect.com
SCIENCE DIRECT®
Journal of Power Sources 144 (2005) 220–225
JOURNAL OF POWER SOURCES
www.elsevier.com/locate/jpowsour

Short communication

Microwave-assisted synthesis of SnO_2–graphite nanocomposites for Li-ion battery applications

Yong Wang, Jim Yang Lee*

Department of Chemical and Biomolecular Engineering, National University of Singapore, 10 Kent Ridge Crescent, 119260 Singapore, Singapore

Received 3 September 2004; accepted 22 December 2004
Available online 16 February 2005

Abstract

SnO_2–graphite nanocomposites are prepared by urea-mediated homogeneous hydrolysis of $SnCl_4$. Heating in a CEM Discover microwave reactor (Sn–C-1), in a household microwave oven (Sn–C-2), or by a conventional conduction method (Sn–C-3) are used to decompose the urea and release hydroxide ions for $SnCl_4$ hydrolysis. The nanocomposites are characterized by XRD, ICP, FE-SEM, SEM and TEM/SAED and used as the material for negative electrodes (anodes) in Li-ion batteries. The SnO_2 particles in Sn–C-1 are the smallest and have the narrowest size distribution (1–3 nm, mean: 2.1 nm, standard deviation: 0.3 nm) compared with those in Sn–C-2 (2–5 nm, mean: 3.8 nm, standard deviation: 0.5 nm) and Sn–C-3 (3–9 nm, mean: 6.4 nm, standard deviation: 0.9 nm). The microwave preparation allows smaller SnO_2 particles to be produced and more homogenously dispersed in the graphite. This results in improved electrochemical performance as a lithium storage compound. The specific capacities decrease in the order: Sn–C-1 > Sn–C-2 > Sn–C-3. For the 14.2 wt.% SnO_2–graphite composite (Sn–C-1), the initial specific capacity was 465 mAh g^{-1} and 80% of the initial specific capacity, or 372 mAh g^{-1} can still be obtained after 60 charge and discharge cycles.

Keywords: Tin oxide; Graphite; Lithium-ion battery; Microwave

1. Introduction

Tin-based lithium storage compounds are most noted for their reasonably low potentials for Li^+ insertion and high storage capacities on both a gravimetric and a volumetric basis [1–4]. On the other hand, poor cycleability remains a serious application issue. Such material deficiency is due to the large specific volume changes during Li^+ insertion and extraction reactions, which causes electrode disintegration. Several research groups have attempted to use Sn, SnO or SnO_2 in conjunction with a carbonaceous material to ease the capacity fading [5–15]. It is believed that both the particle size and size distribution are important factors that affect the material performance. Generally, smaller particles and a more uniform distribution of the particles tend to experience more moderate volume changes and a stable microstructure and, thereby, give improved performance.

Microwave syntheses have been increasingly used in the preparation of high monodispersity nanoparticles of oxides (e.g., SnO_2, CeO_2 and ZrO_2) [16–18] and metals (e.g., Pt, Ru, and Ag) [19–21]. We have produced carbon-supported Pt electro catalysts for fuel cells that have small Pt particle size and a narrow particle-size distribution using microwave radiation coupled with a polyol process [22]. Although the microwave preparation of pristine SnO_2 nanoparticles has been reported [16], the preparation of SnO_2–graphite nanocomposites by microwaves with intended application in Li-ion batteries has not been explored. In this study, we report the microwave synthesis of SnO_2–graphite nanocomposites using two different microwave sources (a CEM Discover microwave reactor and a household microwave oven). This procedures result in good control of both particle size and particle-size distribution. The SnO_2–graphite nanocompos-

* Corresponding author. Tel.: +65 6874 2899; fax: +65 6779 1936.
E-mail address: cheleejy@nus.edu.sg (J.Y. Lee).

0378-7753/$ – see front matter © 2005 Elsevier B.V. All rights reserved.
doi:10.1016/j.jpowsour.2004.12.016

ites exhibit substantially improved physical and electrochemical properties for Li-ion battery applications compared with the same class of composites obtained by conventional conduction heating.

2. Experimental

2.1. Preparation of SnO_2 nanoparticles and SnO_2–graphite nanocomposites (Sn–C-1) by single mode microwave heating

In a 100 ml glass vessel, 0.2 M urea (Aldrich, 98%) was dissolved in 0.1 M $SnCl_4$ (Riedel-de Haen, 99%) aqueous solution to a (mole) ratio of urea to $SnCl_4$ of 4:1. A calculated amount of synthetic graphite (KS6, 19 $m^2\,g^{-1}$) was added to the solution and sonicated for 30 min. The glass vessel was then placed in the cavity of a 300-W CEM Discover microwave reactor. The temperature was ramped from room temperature to 85 °C in 10 s, and the reaction was carried out at this temperature for 3 min with stirring. The resulting suspension, after cooling in an ice bath, was centrifuged at 8000 rpm for 30 min to precipitate the nanocomposites. After washing with a copious amount of distilled water, the precipitate was dried in vacuum at 130 °C overnight and heated in a tube furnace at 600 °C for 3 h on the following day. The resulting product is designated Sn–C-1.

For the preparation of unsupported SnO_2 nanoparticles, graphite was not added to the reaction mixture during preparation. All other steps in the preparation and in the recovery of the solid phase were the same as those for sample Sn–C-1.

2.2. Preparation of SnO_2–graphite nanocomposites (Sn–C-2) by multi-mode microwave heating

The preparation of Sn–C-2 was similar to Sn–C-1, except that a household microwave oven (National NN-S327WF, 2450 MHz, 700 W) was used in lieu of the CEM Discover and the reactants were heated in the microwave oven with medium power for 60 s.

2.3. Preparation of SnO_2–graphite nanocomposites (Sn–C-3) by conventional heating

Sample Sn–C-3 was prepared using the same amounts of reactants as in the preparation of sample Sn–C-1. The reactant suspension was heated in a constant temperature water bath at 85 °C for 3 h. Other than that, all post-processing steps were replicates of the preparation of sample Sn–C-1.

2.4. Electrochemical tests

A *N*-methyl pyrrolidinone (NMP) slurry consisting of 80 wt.% of the composite powder (various samples) and 10 wt.% each of carbon black (Super-P) and polyvinylidene difluoride (Aldrich) was uniformly applied on a copper foil (0.7 mm). The coated foil was cut into disk electrodes with diameters of 11 mm. The electrodes were vacuum dried overnight at 130 °C followed by compression at 2.0×10^6 Pa. They were then assembled into lithium test cells using 0.75 mm lithium foils as negative electrodes, microporous polypropylene separators, and an electrolyte of 1 M $LiPF_6$ in a 50:50 (w/w) mixture of ethylene carbonate (EC) and diethyl carbonate (DEC). Cell assembly was carried out in a re-circulating argon glove-box in which the moisture and the oxygen contents were each below 1 ppm.

All cells were tested galvanostatically at the current density of 0.4 mA cm^{-2} and were charged (Li^+ insertion) and discharged (Li^+ extraction) between fixed voltage limits (2 V–5 mV) by means of a Maccor Series 2000 battery tester.

2.5. Materials characterizations

The tin contents in the composites were determined by inductively coupled plasma (ICP) spectroscopy. Powder X-ray diffraction (XRD) was performed on a Siemens D6000 diffractometer. Particle morphology was examined by means of scanning electron microscopy a (SEM; JEOL JSM-5600LV) by field emission scanning electron microscopy (FE-SEM; JEOL JSM-6700F), and by transmission electron microscopy (TEM; JEOL JEM-2010).

3. Results and discussion

3.1. Preparation and characterization of materials

Tin oxide powders with particle sizes larger than 100 nm are routinely prepared by adding OH^- ions to a tin solution and recovering the precipitate [5,6]. The formation of smaller and nanometer range SnO_2 particles requires the slow and uniform release of OH^- ions to the tin ions. This can be implemented effectively through the thermal decomposition of urea at about 85 °C, as follows [23]:

$$(NH_2)_2CO + 3H_2O \rightarrow CO_2 + 2NH_4^+ + 2OH^- \quad (1)$$

The tin ions in the solution are precipitated as hydrous SnO_2 particles by the action of the in situ generated OH^- ions.

In this work, the heat required for urea thermolysis came from three different sources. The first two sources were based on microwave irradiation using a single mode CEM Discover reactor and a household multimode microwave oven, respectively. The third source was conduction heating in a water bath. TEM images of 14.2 wt.% (Sn–C-1), 14.9 wt.% (Sn–C-2) and 14.4 wt.% (Sn–C-3) SnO_2–graphite nanocomposites prepared from these different heat sources are shown in Fig. 1. The tin contents in the composites were determined by ICP, and reported as elemental tin. All the prepared SnO_2 particles were in the sub-10 nm range, and were much smaller than SnO_2 particles prepared from a non-mediated hydrolysis route [5,6]. The particle-size dis-

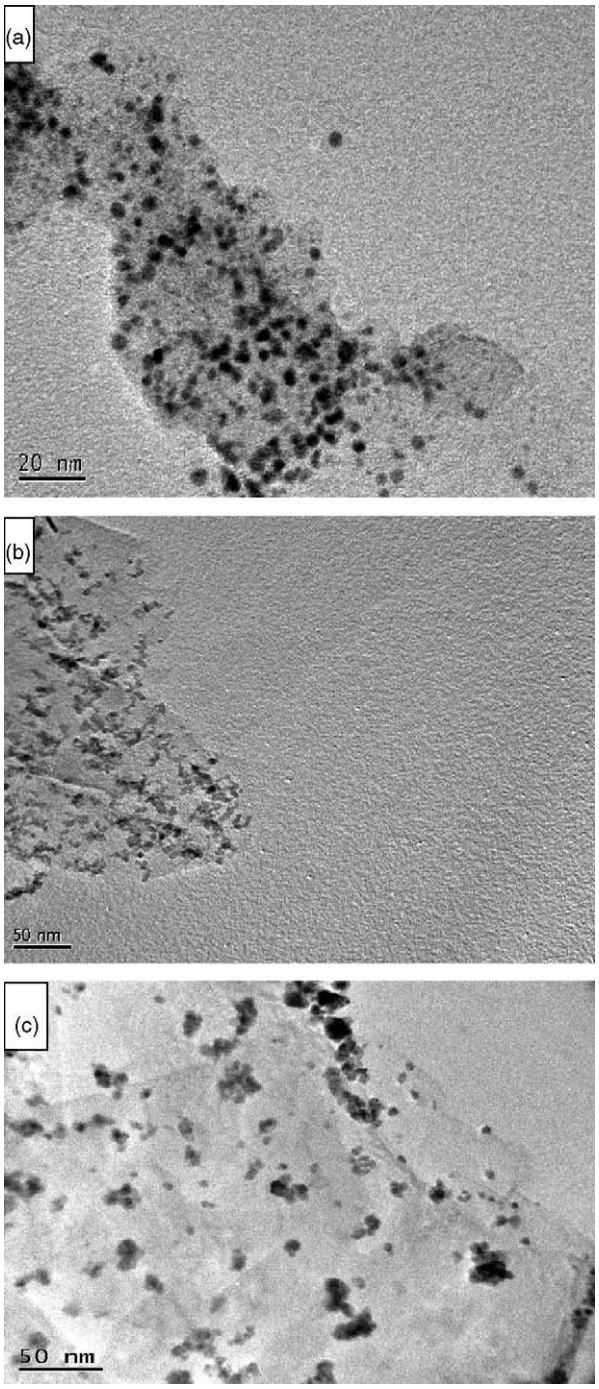

Fig. 1. TEM images of various SnO_2–graphite nanocomposites: (a) Sn–C-1, (b) Sn–C-2, (c) Sn–C-3.

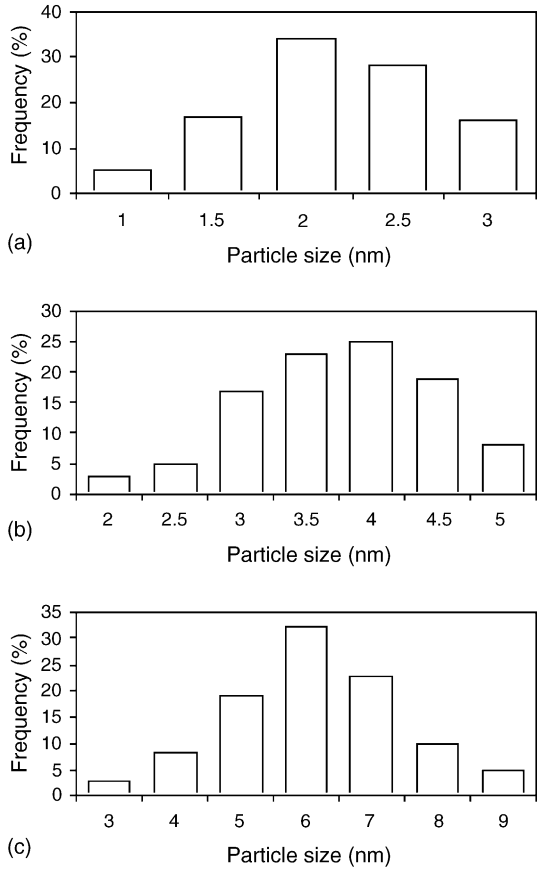

Fig. 2. Particle-size distributions from TEM measurements of: (a) Sn–C-1, (b) Sn–C-2, (c) Sn–C-3.

tributions of the three SnO_2–graphite nanocomposites, using statistics generated from randomly chosen areas in the TEM images, are shown in Fig. 2. More than 100 nanoparticles were counted in each instance. There were significant differences between the three nanocomposites in terms of particle size and particle-size distribution. In general, the microwave-synthesized SnO_2–graphite nanocomposites (Sn–C-1 and Sn–C-2) had smaller SnO_2 particles and narrower particle-size distributions (Sn–C-1: 1–3 nm, mean = 2.1 nm, standard deviation = 0.3 nm; Sn–C-2: 2–5 nm, mean = 3.8 nm, standard deviation = 0.5 nm) than those prepared by conduction heating (Sn–C-3: 3–9 nm, mean = 6.4 nm, standard deviation = 0.9 nm).

Microwaves are electromagnetic radiations with mutually perpendicular electric and magnetic field components. The rotational motion of polar molecules in attempting to align themselves with the rapidly changing electric field, and the ionic motion in microwave-susceptive materials, are two fundamental mechanisms of energy transfer from microwaves to materials. According to the generalized mechanism of metal oxide formation under microwave irradiation [16,17], the Sn^{4+} complexes with H_2O molecules or OH^- ions, viz., $Sn(H_2O)_x(OH)_y^{(4-y)+}$, tend to lose protons by the action of H_2O. Since water is a solvent with a very high dipole moment, microwave irradiation may be used to accelerate the de-protonation reaction, as shown by:

$$Sn(H_2O)_x(OH^-)_y^{(4-y)+} + H_2O \rightarrow SnO_2 \cdot nH_2O + (H_3O)^+ \quad (2)$$

The fast heating by microwaves accelerates the hydrolysis reaction, and hence the nucleation of the oxides. Microwave also reduces the temperature and concentration gradients in the reaction medium, and thereby provides a more homoge-

nous environment for chemical reactions and particle growth. Subsequently, smaller particles with a narrower particle-size distribution are more accessible by microwave heating than by conduction heating.

It is also noted that the SnO_2 nanoparticles in sample Sn–C-1 are smaller than those in sample Sn–C-2. In the household microwave oven, the reaction temperature was close to the boiling point of water (100 °C) because of the lack of an external means of temperature control. In the CEM microwave reactor, however, the temperature could be held constant at 85 °C, which is more suitable for the slow decomposition of urea, through feedback control and adjustment of the radiation power level. It is reasonable to assume that the urea decomposition rate should increase with temperature. In addition, the CEM Discover is a focused-beam microwave reactor, which offers concentrated microwave irradiation on the reactants. Controllable ramp time, hold time (reaction time), and uniform stirring are only available with the CEM microwave reactor. All of these parameters could be adjusted to provide a reproducible and homogeneous reaction environment that was conducive to the formation of smaller and more uniform nanoparticles.

The TEM image in Fig. 3(a) shows the as-prepared and unsupported hydrous SnO_2 nanoparticles from the CEM microwave reactor to be heavily agglomerated particles of 1–3 nm. The corresponding selected area, electron diffraction pattern (SAED) shown as an inset indicates that the oxide is amorphous at this stage. After calcination at 600 °C for 3 h, there is a noticeable increase in the particle size to 1–8 nm (Fig. 3b) as expected from the condensation of hydroxyl groups pulling the particles together [24]. Particle growth in calcination is more uninhibited than the case of sample Sn–C-1, because of the lack of the graphite support. The SAED pattern of unsupported SnO_2 nanoparticles indicates that the SnO_2 nanoparticles are crystalline after calcination. Several major fringe patterns with interplanar distances of 3.35, 2.64, 1.76, and 1.42 Å can be identified in the electron diffraction patterns, and correspond well with the (1 1 0), (1 0 1), (2 1 1) and (3 0 1) diffractions of tetragonal cassiterite, or tin oxide with the rutile structure. The SEM images of tin oxide nanoparticles with and without the graphite support in Fig. 4 are in qualitative agreement with the TEM examination of these samples.

The XRD patterns of as-prepared and calcined SnO_2 nanoparticles using the CEM microwave reactor are presented in Fig. 5. The as-prepared SnO_2 nanoparticles are amorphous before the heat treatment. Characteristic peaks (1 1 0, 1 0 1, 2 0 0, 2 1 1, 2 2 0, 3 1 0, 1 1 2 and 3 0 1) of SnO_2 only appeared after the unsupported SnO_2 nanoparticles are calcined at 600 °C. The peak positions agree well with previously reported values of SnO_2 diffractions (JCPDS 41-1445).

3.2. Materials electrochemical properties

The first cycle of Li insertion and extraction for samples Sn–C-1 and Sn–C-3 prepared by microwave synthesis

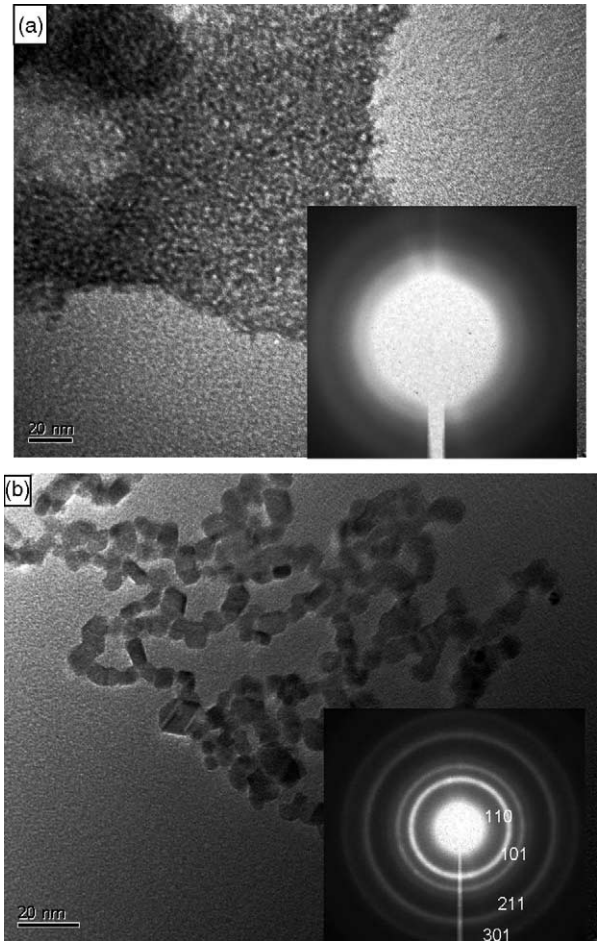

Fig. 3. TEM images of products from CEM microwave reactor: (a) as-prepared hydrous SnO_2 nanoparticles with an inset showing the corresponding SAED pattern; (b) pristine SnO_2 nanoparticles after calcination with an inset showing corresponding SAED.

(in the CEM reactor) and conduction heating are given in Fig. 6. Cycling was performed at a constant current density of 0.4 mA cm^{-2} (approximating the C/6 rate) with cut-off potentials at 5 mV and 2 V versus Li/Li^+. The two curves are very similar, with a small but detectable voltage plateaux found near 0.85 V. The charge uptake at 0.85 V and above has been investigated extensively, and can be assigned to the reduction of SnO_2 and the formation of solid electrolyte interface (SEI) layers on graphite and on the nascent Sn surface [1].

The cycleability of graphite-supported SnO_2 nanoparticles [Sn–C-1 (14.2 wt.% SnO_2), Sn–C-2 (14.9 wt.% SnO_2), and Sn–C-3 (14.4 wt.% SnO_2)] prepared by microwave synthesis in the CEM reactor, in the household microwave oven, and by conduction heating, respectively, is compared in Fig. 7(a). The initial specific capacity of Sn–C-1 is found to be 465 mAh g^{-1}, which is a value much higher than the weighted sum of the specific capacities of graphite (300 mAh g^{-1}) and pristine SnO_2 (645 mAh g^{-1}) measured under identical test conditions. This indicates that the nanocomposite is not simply an intimate physical mixture

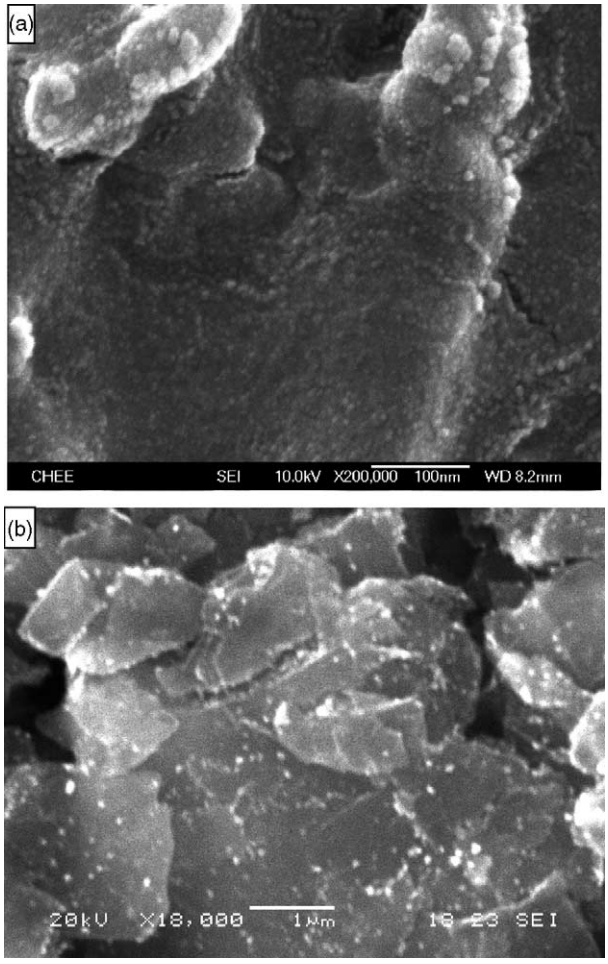

Fig. 4. FE-SEM/SEM images of (a) tin oxide nanoparticles and (b) 14.2 wt.% tin oxide–graphite nanocomposites from CEM microwave reactor.

of the two components. Presented in another way, Fig. 7(b) shows the SnO_2 contribution to the overall capacities assuming that KS6 delivered a constant capacity of 300 mAh g^{-1} (experimental value, since fading was measured to be <6% in 60 cycles for KS6 alone) throughout cycling. The following equation is used to calculate the SnO_2 capacities.

$$\text{capacity of } SnO_2 = \frac{\text{capacity of composite} - 300 \times (\text{carbon weight fraction})}{SnO_2 \text{ weight fraction}} \quad (3)$$

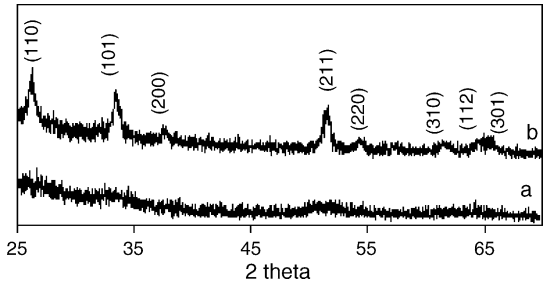

Fig. 5. X-ray powder diffraction patterns of (a) as-prepared hydrous SnO_2 and (b) pristine SnO_2 after calcinations from CEM microwave reactor.

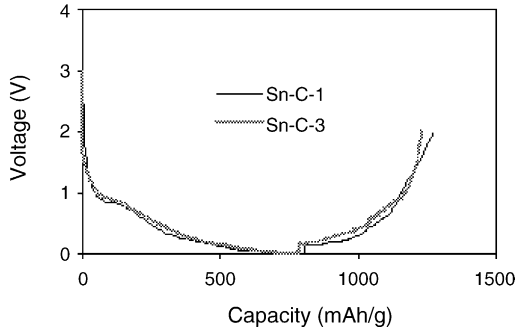

Fig. 6. First lithiation and de-lithiation cycles of sample Sn–C-1 and Sn–C-3.

The calculated SnO_2 capacities (Sn-1, Sn-2, and Sn-3) in the three composites (Sn–C-1, Sn–C-2, and Sn–C-3) are all above 1400 mAh g^{-1} initially, which exceeds the theoretical capacity of SnO_2 (~790 mAh g^{-1}). The carbon-supported SnO_2 nanoparticles therefore show a substantial capacity advantage relative to the individual components. The capacity increase over the weighted sum may originate from disordering of the graphite structure, a feature that is known to store more Li ions [8].

The initial specific capacities of sample Sn–C-2 and Sn–C-3 are similar, at 472 and 460 mAh g^{-1}, respectively. On the other hand, the cycleability of the microwave-derived samples (Sn–C-1 and Sn–C-2) is much better than that of the Sn–C-3 sample produced by conduction heating. For the two microwave-derived samples, Sn–C-1 cycled noticeably better than Sn–C-2. The initial specific capacities of Sn–C-1 and Sn–C-2 decrease by 10 and 11% after 40 cycles and by 20 and 25% after 60 cycles, respectively. The corresponding decreases for Sn–C-3 are 26 and 44%, i.e., nearly

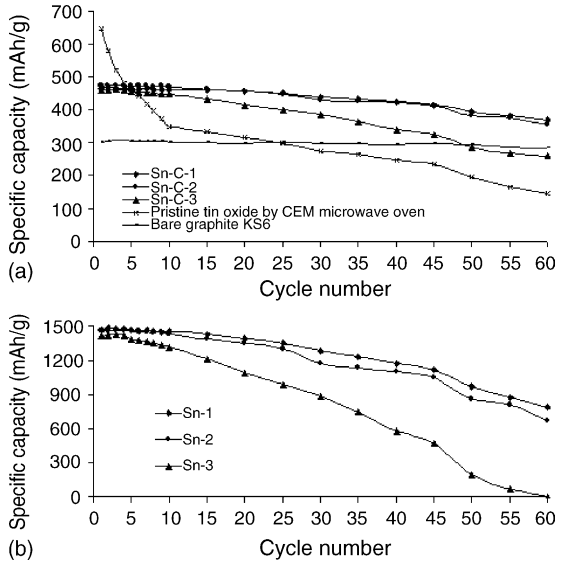

Fig. 7. Cycleability of (a) various SnO_2 modified graphite composite electrodes and (b) SnO_2 contributions in various composites assuming constant KS6 capacity of 300 mAh g^{-1} (0.4 mA cm^{-2}, 5 mV–2 V) throughout cycling.

double the microwave values. It should perhaps be emphasized that the cycleability of these two microwave-derived samples in the absence of PVP is an improvement over the carbon-supported and PVP-protected SnO_2 nanoparticles prepared by urea mediated hydrolysis in a water bath [15]. The samples obtained by combining urea mediated hydrolysis and microwave heating represent a notable improvement for SnO_2-based Li storage materials, although in its present form the procedure is still unable to address fully the cycleability issue associated with the use of SnO_2. The rate of agglomeration of Sn nanoparticles that leads to the loss of utilization during cycling may be reduced through the use of small particles [25], but is not completely eradicated. Therefore, control of the particle size of tin only offers a partial solution to the cycleability issue. More research is required before tin-based anodes can be commercially adopted.

4. Conclusions

A single-mode microwave reactor (CEM Discover), a household microwave oven and conduction heating have been used in the preparation of SnO_2 nanoparticles by means of urea-mediated hydrolysis of $SnCl_4$. Synthetic graphite KS6 is introduced during the preparation to obtain SnO_2–graphite composites. The resulting SnO_2 nanoparticles and KS6 supported SnO_2 nanoparticles have been extensively characterized. The SnO_2 particles in a sample (Sn–C-1) prepared in the CEM microwave reactor have the smallest (1–3 nm) diameter and the most uniform particle-size distribution (mean = 2.1 nm, standard deviation = 0.3 nm). The sample delivers the best cycleability among the three SnO_2–graphite composites prepared in this study because of the good control of the size and the size distribution of the particles.

References

[1] I.A. Courtney, J.R. Dahn, J. Electrochem. Soc. 144 (1997) 2045–2052.
[2] A.H. Whitehead, J.M. Elliott, J.R. Owen, J. Power Sources 81 (1999) 33–38.
[3] A.S. Yu, R. Frech, J. Power Sources 104 (2002) 97–100.
[4] Y.N. Nuli, S.L. Zhao, Q.Z. Qin, J. Power Sources 114 (2003) 113–120.
[5] J.Y. Lee, R.F. Zhang, Z.L. Liu, Electrochem. Solid-State Lett. 3 (2000) 167–170.
[6] J.Y. Lee, R.F. Zhang, Z.L. Liu, J. Power Sources 90 (2000) 70–75.
[7] J. Read, D. Foster, J. Wolfenstine, W. Behl, J. Power Sources 96 (2001) 277–281.
[8] G.X. Wang, J.H. Ahn, M.J. Lindsay, L. Sun, D.H. Bradhurst, S.X. Dou, H.K. Liu, J. Power Sources 97/98 (2001) 211–215.
[9] M. Egashira, H. Takatsuji, S. Okada, J. Yamaki, J. Power Sources 107 (2002) 56–60.
[10] J.K. Lee, D.H. Ryu, J.B. Ju, Y.G. Shul, B.W. Cho, D. Park, J. Power Sources 107 (2002) 90–97.
[11] L.H. Shi, H. Li, Z.X. Wang, X.J. Huang, L.Q. Chen, J. Mater. Chem. 11 (2001) 1502–1505.
[12] B. Veeraraghavan, A. Durairajan, B. Haran, B. Popov, R. Guidotti, J. Electrochem. Soc. 149 (2002) A675–A681.
[13] Y. Liu, J.Y. Xie, Y. Takeda, J. Yang, J. Appl. Electrochem. 32 (2002) 687–692.
[14] Y. Wang, J.Y. Lee, B.H. Chen, Electrochem. Solid-State Lett. 6 (2003) A19–A22.
[15] Y. Wang, J.Y. Lee, Electrochem. Commun. 5 (2003) 292–296.
[16] J.J. Zhu, J.M. Zhu, X.H. Liao, J.L. Fang, M.G. Zhou, H.Y. Chen, Mater. Lett. 53 (2002) 12–19.
[17] X.H. Liao, J.M. Zhu, J.J. Zhu, J.Z. Xu, H.Y. Chen, Chem. Commun. (2001) 937–938.
[18] J.H. Liang, Z.X. Deng, X. Jiang, F. Li, Y. Li, Inorg. Chem. 41 (2002) 3602–3604.
[19] W.Y. Yu, W.X. Tu, H.F. Liu, Langmuir 15 (1999) 6–9.
[20] W.X. Yu, H.Y. Liu, Chem. Mater. 12 (2000) 564–567.
[21] W.X. Tu, H.F. Liu, J. Mater. Chem. 10 (2000) 2207–2211.
[22] W.X. Chen, J.Y. Lee, Z. Liu, Chem. Commun. (2002) 2588–2589.
[23] K.C. Song, Y. Kang, Mater. Lett. 42 (2000) 283–289.
[24] N.L. Wu, S.Y. Wang, I.A. Rusakova, Science 285 (1999) 1375–1377.
[25] H. Li, L.H. Shi, W. Lu, X.J. Huang, L.Q. Chen, J. Electrochem. Soc. 148 (2001) A915–A922.